two consecutive stages have been identified. In the first stage (373-673 K), the decrease of hydrogen adsorption is accompanied by an incorporation of hydrogen into the support.[27] After the hydrogen is removed by outgassing of the sample at 773 K, metal particles recover their initial electronic properties and adsorption capacity.[28] In the second stage (above 673 K), the incorporated hydrogen is eliminated and two new factors responsible for adsorption suppression are operating: (i) physical blocking by TiO_x species of metal adsorption sites and (ii) electronic perturbation of the metal, due to formation of rhodium-titanium bonds between metal particles and TiO_x species and/or reduced support.[7-9,11] The effect of both phenomena increases with temperature and time of reduction, but their relative contribution depends on reduction conditions. Adsorption suppression due to electronic perturbation of the metal is enhanced in dynamic reductions while physical blocking is not appreciably affected by the type of reduction. In static conditions the small electronic contribution makes physical blocking the preferentially detected effect. The electronic perturbation is eliminated by oxidation of the sample at 473 K, but removal of TiO_x species from the metal requires that oxidation be carried out at 673 K.[30] In this case electronic properties and adsorption capacity of the metal are completely recovered.

Acknowledgment. This research was supported by Grants MAT 88-0223 and MAT 91-1080 from the Comision Interministerial de Ciencia y Tecnologia (CICYT). J.P.B. thanks the Ministerio de Educación y Ciencia of Spain for a postgraduate fellowship. We thank C. Alonso, I. Sobrados, and T. G. Somolinos for helpful technical assistance.

Registry No. Rh, 7440-16-6; TiO_2, 13463-67-7; H_2, 1333-74-0.

Adsorption and Decomposition of Acetylene on Si(100)-(2×1)

P. A. Taylor,[†] R. M. Wallace,[‡] C. C. Cheng,[†] W. H. Weinberg,[§] M. J. Dresser,[∥] W. J. Choyke,[⊥] and J. T. Yates, Jr.*,[†]

Contribution from the Surface Science Center, Department of Chemistry, University of Pittsburgh, Pittsburgh, Pennsylvania 15260. *Received December 16, 1991*

Abstract: The adsorption and decomposition of acetylene on Si(100)-(2×1) have been studied in ultrahigh vacuum by Auger electron spectroscopy, temperature-programmed desorption, and changes in the partial pressure of acetylene as measured by a quadrupole mass spectrometer during the formation of a monolayer. Acetylene was found to chemisorb onto Si(100)-(2×1) via a mobile precursor. The difference between the activation energy for desorption from the precursor and that for reaction from the precursor into the chemisorbed state was found to be $(E_d - E_r) = 1.9 \pm 0.6$ kcal mol^{-1}. At a low surface temperature, reaction from the precursor state dominates, giving a chemisorption probability of unity at submonolayer coverages. The saturated acetylene coverage is measured to be one C_2H_2 per Si_2 dimer. Thermochemical arguments are presented, which indicate that acetylene bonds as a di-σ species to dimer sites in which the Si-Si dimer bond has been cleaved. Chemisorbed acetylene was found to undergo two thermal reactions. A minor pathway (<5%) involves acetylene desorption, and a major pathway (>95%) involves the dissociation of acetylene to produce chemisorbed carbon and H_2 (g). At temperatures above 800 K, the surface carbon begins to diffuse into the bulk of the silicon crystal.

I. Introduction

The interaction of hydrocarbons with silicon surfaces forms the basis for various technological processes for the production of silicon carbide films.[1-5] The processes of chemical vapor deposition[1-3] and plasma deposition[4,5] of silicon carbide films involve elementary chemical reactions which have not been elucidated in detail, even for simple hydrocarbon reactants.

While chemical vapor deposition (CVD) involves the interaction of gas-phase reactants with surfaces which are heated, it is important to study adsorption at low surface temperatures in order to separate reactions of low activation energy (such as surface migration and adsorption) from reactions of higher activation energy (such as C-H and C-C bond scission in the chemisorbed species). All of these reactions are involved in CVD processes at high temperatures.

At low temperatures, silicon interacts differently with the C-C σ-bonds of saturated hydrocarbons and the C-C π-bonds of unsaturated hydrocarbons.[6] Saturated hydrocarbons do not chemisorb on Si(100) at low temperatures. Unsaturated molecules such as ethylene and propylene chemisorb with high probability and with strong bonding on Si(100).[7,8] In this paper we extend the study of unsaturated hydrocarbon chemistry on Si(100) to acetylene.

Acetylene, like propylene and ethylene, adsorbs with high probability on Si(100) at 105 K; upon heating, approximately 95% of the chemisorbed acetylene thermally dissociates on the surface. This is accompanied by the desorption of hydrogen and the retention of carbon adatoms which diffuse into the bulk silicon above approximately 800 K. The diffusion of carbon adatoms into the silicon lattice forms a layer which will be referred to as "Si-C", which may be viewed as a precursor to the CVD growth of silicon carbide. The remaining 5% of acetylene desorbs without decomposition with an activation energy indicative of strong chemical bonding of chemisorbed acetylene.

[†] Department of Chemistry, University of Pittsburgh.
[‡] Present address: Texas Instruments, Inc., Central Research Laboratories, MS147, Dallas, TX 75265.
[§] Present address: Department of Chemical Engineering, University of California, Santa Barbara, CA 93106.
[∥] Present address: Department of Physics, Washington State University, Pullman, WA 99163.
[⊥] Present address: Department of Physics, University of Pittsburgh, Pittsburgh, PA 15260.

(1) Nishino, S.; Powell, J. A.; Will, H. A. *Appl. Phys. Lett.* **1983**, *42*, 460.
(2) Addamiano, A.; Sprague, J. A. *Appl. Phys. Lett.* **1984**, *44*, 525.
(3) Bozso, F.; Yates, J. T., Jr.; Choyke, W. J.; Muehlhoff, L. *J. Appl. Phys.* **1985**, *57*, 2771.
(4) Catherine, Y.; Turban, G.; Grolleau, B. *Thin Solid Films*, **1981**, *76*, 23.
(5) Mahan, A. H.; von Roedern, B.; Williamson, D. L.; Madan, A. *J. Appl. Phys.* **1985**, *57*, 2717.
(6) Bozack, M. J.; Taylor, P. A.; Choyke, W. J.; Yates, J. T., Jr. *Surf. Sci.* **1986**, *177*, L933.
(7) Clemen, L. L.; Wallace, R. M.; Taylor, P. T.; Dresser, M. J.; Weinberg, W. H.; Choyke, W. J.; Yates, J. T., Jr. *Surf. Sci.* **1992**, *268*, 205.
(8) Bozack, M. J.; Choyke, W. J.; Muehlhoff, L.; Yates, J. T., Jr. *Surf. Sci.* **1986**, *176*, 547.

0002-7863/92/1514-6754$03.00/0 © 1992 American Chemical Society

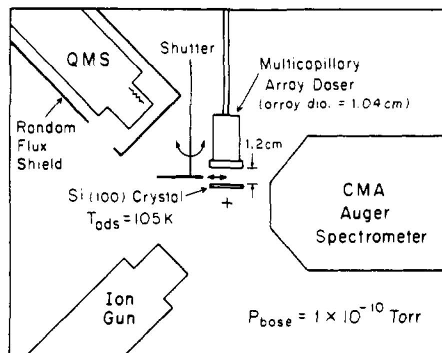

Figure 1. UHV system II: used to measure adsorption kinetics (absolute coverages) of acetylene on Si(100)-(2×1).

II. Experimental Methods

One ultrahigh vacuum (UHV) system (system I) used in these studies (base pressure 1×10^{-10} Torr) has been described previously.[8] The system was equipped with a Varian single-pass CMA Auger electron spectrometer (AES), a Varian ion gun, a collimated gas doser,[9] a UTI-100C quadrupole mass spectrometer (QMS), and a three-grid low-energy electron diffraction/electron-stimulated desorption ion angular distribution (LEED/ESDIAD) apparatus.

Additional studies of the adsorption kinetics of acetylene on Si(100) have been performed in a second ultrahigh vacuum system (system II) equipped with a calibrated gas doser, a movable shutter, and a mass spectrometer shielded from direct line of sight from the crystal (Figure 1). This system contains a PHI CMA Auger electron spectrometer.

A $1.50 \times 1.50 \times 0.15$ cm Si(100) B-doped, 10 Ω cm crystal was used for these studies. The crystal was mounted[9] with tantalum tabs wedged into 0.4-mm slots on two edges of the crystal. The tantalum tabs were welded to tungsten leads, which provide electrical contact for resistive heating as well as thermal contact to a liquid-nitrogen-cooled support block on the manipulator. A chromel–constantan thermocouple (type E, 0.08-mm diameter), spot welded inside a tantalum foil sleeve, was wedged into a third slot in the crystal, providing an accurate means of measuring the crystal temperature. The crystal, in system I, was cleaned by a 1 mm diameter, 2-keV Ar^+ beam rastered across the crystal at a glancing angle 70° from the crystal normal with a current of 2–4 μA at the crystal for 30–60 min followed by annealing to 1190 K. Auger spectroscopy showed no detectable surface impurities after this sputter–anneal treatment. Occasionally, LEED measurements were made on the crystal following the sputter–anneal procedure giving a sharp, reproducible reconstructed Si(100)-(2×1) LEED pattern. In system II, the cleaning procedure involved sputtering with 2-keV Ar^+ ions at normal incidence to the crystal, with a current of 2.5 μA for 60 min, followed by annealing to 1100 K for 15 min.

Auger scans in system I were taken using a primary energy of E_p = 3 kV and a modulation voltage of V_m = 10 V. The electron current at the crystal under normal operating conditions was 5 μA, focused into a beam estimated to be 0.2-mm in diameter. The Auger peak-to-peak height ratio H(noise)/H(Si(LVV)) was approximately ~0.02 for a clean Si(100) crystal. Auger intensity ratios reported before and after desorption experiments, to be described, represent the average of measurements at six different points on the crystal.

It is well-known that adsorbed hydrocarbons on Si(100) are subject to electron-beam damage during Auger measurements.[8] The cross section for electron-induced decomposition of propylene on Si(100) is $\sim 4 \times 10^{-18}$ cm^2 for 20-eV electrons.[8] In the Auger measurements reported here, in system I, the focused ~0.2 mm diameter beam corresponds to an electron flux of $\sim 1 \times 10^{17}$ e cm^{-2} s^{-1}. During a single AES measurement (with a scan time of 120 s) the electron fluence was $\sim 1.2 \times 10^{19}$ e cm^{-2}. Due to the large fluence of electrons at the crystal, all adsorbed hydrocarbons in the AES electron beam will have decomposed by electron-stimulated processes leaving adsorbed carbon. Separate electron stimulated desorption (ESD) studies (data not shown), however, have shown no significant decrease in the carbon Auger peak-to-peak intensity during the course of the Auger measurement. Therefore, the reported C(KLL) Auger peak-to-peak measurements are an assay of the surface carbon concentration originating from the adsorbed acetylene and hence are proportional to the coverage of adsorbed acetylene.

Adsorption of C_2H_2 on the Si(100) crystal was accomplished either by rotating the clean crystal into an acetylene beam (system I) or by rapidly removing a shutter between the crystal and the microcapillary array gas doser delivering a beam of acetylene (system II). The flow rate from the doser was controlled by establishing a known C_2H_2 pressure behind a conductance-limiting 2 μm diameter orifice inside the doser assembly. Details of the gas-handling system and doser assembly are given elsewhere.[9] In system II, the conductance measurements of three separate gases gave an accurate estimate of $(2.51 \pm 0.12) \times 10^{-4}$ cm^3 s^{-1} for the acetylene conductance through the orifice.[10] For acetylene, the pressure-dependent flow rate through the doser was calculated to be 8.08×10^{12} C_2H_2 molecules Torr^{-1} s^{-1}. The results of a typical adsorption experiment from system II with a C_2H_2 backing pressure of 0.50 Torr are shown in Figure 2. With the crystal-doser geometry shown in Figure 1, a fraction of the gas flux misses the crystal, and a calculated geometrical factor of 0.46 ± 0.05 was obtained to convert the exiting flow from the doser to the flux arriving at the Si(100) crystal.[11] Assuming a probability of adsorption of unity at 105 K, an experimental geometrical factor may be obtained[10,12] from the ratio of the initial QMS signal of acetylene with the shutter blocking the crystal, $(\Delta_1 + \Delta_2)$, and with the shutter removed, Δ_2, allowing the C_2H_2 to adsorb on the Si(100) crystal, as shown in Figure 2. From a number of adsorption measurements such as that shown in Figure 2, an experimental geometrical factor of $\Delta_1/(\Delta_1 + \Delta_2) = 0.45 \pm 0.01$ was obtained. This is in excellent agreement with the calculated value of 0.46 ± 0.05. The gentle slope of the background curve is mainly related to wall effects as they relate to C_2H_2 molecules which have missed the crystal or are reflected by the crystal.

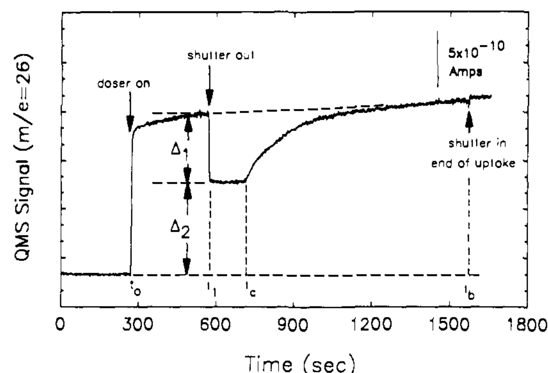

Figure 2. Adsorption kinetics of acetylene on Si(100)-(2×1) at 105 K. The geometric correction factor used to experimentally measure the flux at the crystal is $\Delta_1/(\Delta_1 + \Delta_2)$.

The acetylene (99.6%) was supplied by Matheson. Since acetylene is shipped dissolved in acetone, special care was taken to remove all traces of acetone. To purify the acetylene, 760 Torr of acetylene was transferred from the cylinder to a glass bulb using a glass vacuum system with a base pressure of 1×10^{-7} Torr. The acetylene in the glass bulb was first frozen with liquid nitrogen, and any dissolved air was pumped away. Afterward, the acetylene in the bulb was allowed to thaw. Next, the acetylene was frozen with a cyclohexene–liquid nitrogen slurry at 169 K. At 169 K acetone has no appreciable vapor pressure while the vapor pressure of acetylene is approximately 140 Torr. This temperature allows the acetone to remain in the first bulb while the pure acetylene is frozen in a second bulb at 77 K. This procedure produced acetylene free of impurities, which was confirmed by mass spectra. In particular, the base peak of acetone, CH_3CO^+ (m/e = 43), indicated that any acetone impurity was below 0.05%.

Thermal desorption spectra were recorded with a multiplexed QMS driven by a Teknivent mass spectral data system.[8] During temperature-programmed desorption, in system I, the exposed crystal surface was perpendicular to the axis of the QMS ionizer and at a distance of 4 cm. The mass peaks monitored during desorption were mass 26 ($C_2H_2^+$), mass 13 (CH^+), and mass 2 (H_2^+). A temperature ramp between 110 and 1000 K was provided by a Honeywell UDC 500 temperature controller used to drive a feedback circuit to control the power to the crystal.[13] The controller was capable of producing a reproducible temper-

(9) Bozack, M. J.; Muehlhoff, L.; Russell, J. N., Jr.; Choyke, W. J.; Yates, J. T., Jr. *J. Vac. Sci. Technol.* **1987**, *A5*, 1.

(10) Cheng, C. C.; Wallace, R. M.; Taylor, P. A.; Choyke, W. J.; Yates, J. T., Jr. *J. Appl. Phys.* **1990**, *67*, 3693.

(11) (a) Campbell, C. T.; Valone, S. M. *J. Vac. Sci. Technol.* **1985**, *A3*, 408. (b) Winkler, A.; Yates, J. T., Jr. *J. Vac. Sci. Technol.* **1988**, *A6*, 2929.

(12) Smentkowski, V. S.; Yates, J. T., Jr. *J. Vac. Sci. Technol.* **1989**, *A7*, 3325.

(13) Muha, R. J.; Gates, S. M.; Yates, J. T., Jr.; Basu, P. *Rev. Sci. Instrum.* **1985**, *56*, 613. The temperature controller used to ramp the silicon crystal differs from the controller described by Muha et al. in two aspects: (1) The thermocouple amplifier and ramp generator have been incorporated into the Honeywell process controller. (2) The power driver has a feedback loop that monitors power.

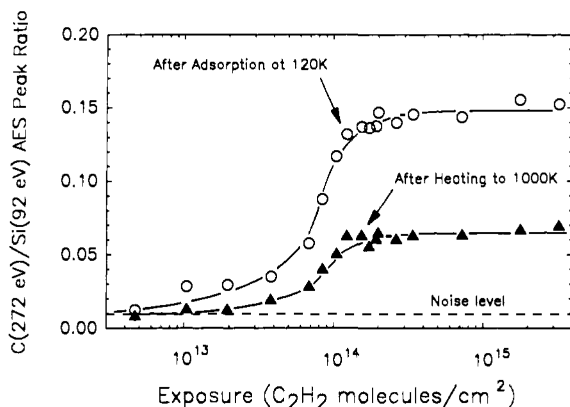

Figure 3. C(KLL)/Si(LVV) Auger ratios after adsorption of acetylene on Si(100) and after temperature-programmed desorption. The maximum temperature during desorption is 1000 K where extensive carbon penetration into the silicon crystal has occurred.

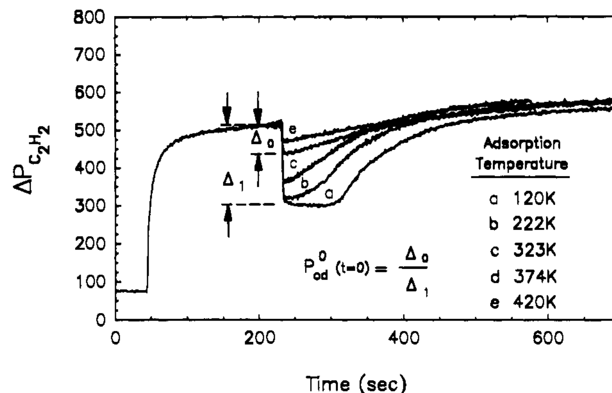

Figure 4. Rate of adsorption of acetylene on Si(100) at different surface temperatures. A decrease in the initial adsorption probability, P_{ad}^0, is observed as the surface temperature increases.

ature ramp, and in the region between 450 and 900 K, which is of particular interest in this paper, the controller gave a linear temperature ramp of $dT/dt = 0.87$ K s^{-1}.

In some experiments, atomic hydrogen was used as a reactant. This was produced by a tungsten filament maintained at 1800 K, with line of sight to the Si(100) crystal. The filament was employed in a H_2 background pressure of $\sim 1 \times 10^{-8}$ Torr (uncorrected ion gauge).

III. Results

A. Adsorption of Acetylene at 105 K. The adsorption of acetylene onto Si(100)-(2×1) at 105 K is indicated by the drop in the mass spectrometric intensity for mass 26 upon removing the shutter between the beam of C_2H_2 and the Si(100) crystal, as shown in Figure 2. The initial drop is followed by a region of constant C_2H_2 intensity (t_1 to t_a in Figure 2) indicating a constant probability of adsorption of C_2H_2 on Si(100) at 105 K. This region of constant uptake rate terminates at t_a in Figure 2. Beyond t_a the acetylene background pressure slowly rises indicating that the net rate of acetylene adsorption is continuously decreasing as the crystal exposure to C_2H_2 increases. The agreement between the calculated geometrical factor (0.46 ± 0.05) and the experimentally measured geometrical factor (0.45 ± 0.01) indicates that the initial probability of adsorption of acetylene on Si(100) is approximately unity. Furthermore, the observation of a *constant* probability of adsorption over a wide initial coverage range (t_1–t_a in Figure 2) also supports the fact that the probability of adsorption is unity in this coverage range.

Auger spectroscopic measurements were also employed to study the kinetics of C_2H_2 adsorption on Si(100) at 120 K, using system I in which our absolute C_2H_2 exposure scale is not so well-defined as in system II. In Figure 3 the growth of the C(KLL)/Si(LVV) Auger ratio is plotted as a function of C_2H_2 exposure. Measurements of each point were made in separate adsorption experiments to avoid the possibility of cumulative errors due to electron-beam effects in the Auger measurements. The sharp increase in the C(KLL)/Si(LVV) ratio occurs over the exposure range where the adsorption probability $P_{ad} = 1$, in the region of t_1–t_a in the adsorption-uptake curve (Figure 2).

In addition to the adsorption curve plotted in Figure 3, the Si(100) crystal at each coverage was heated to 1000 K at a rate of ~ 1 K s^{-1}, to cause desorption and decomposition of C_2H_2 (a), and immediately quenched to 120 K at a rate of ~ 5 K s^{-1}. Once at 120 K, a second Auger measurement was performed. These measurements indicate a decrease in the C(KLL)/Si(LVV) ratio due to diffusion of carbon into the silicon lattice, to be discussed below. The Auger line shape for the carbon observed in both adsorption and heating experiments does not change.

B. Temperature Dependence of Adsorption. Above 160 K the probability of adsorption of C_2H_2 on Si(100) varies as a function of the Si(100) surface temperature. The temperature dependence of the rate of adsorption of C_2H_2 on Si(100) is shown by the behavior of the adsorption curves in Figure 4. The kinetics of adsorption may be modeled with a weakly bound precursor state (p) and a strongly bound chemisorption state (c).[14] The adsorption reaction through a precursor state may be expressed as

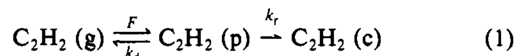

$$C_2H_2\,(g) \underset{k_d}{\overset{F}{\rightleftharpoons}} C_2H_2\,(p) \xrightarrow{k_r} C_2H_2\,(c) \qquad (1)$$

where F is the flux arriving at the crystal in units of molecules site^{-1} s^{-1}, and k_d and k_r are the rate coefficients of desorption and chemisorption, respectively. Here, we shall consider two cases. In case 1, both "intrinsic" and "extrinsic" precursor states exist on the surface and they are energetically equivalent. Since desorption of molecular acetylene is observed from the crystal surface (using the apertured QMS) at high coverages at 140 K, this is probably the most reasonable assumption. In case 2, only intrinsic precursors have a sufficient lifetime to be kinetically relevant. For this situation the resulting expression for the probability of adsorption will be unchanged in the limit of short time from that of case 1. In case 2, the probability of adsorption would decrease more rapidly as a function of surface coverage compared to case 1. Therefore, the rate of adsorption into the chemisorption state as described in case 1 is simply

$$\frac{d\theta_c}{dt} = k_r\theta_p(1 - \theta_c) \qquad (2)$$

where θ_c and θ_p are the fractional coverages of the chemisorbed and both intrinsic and extrinsic precursor species at time t. A similar expression may be written for the rate of adsorption into the precursor state

$$\frac{d\theta_p}{dt} = F\xi - k_d\theta_p - k_r\theta_p(1 - \theta_c) \qquad (3)$$

where ξ is the trapping probability of C_2H_2, which is equal to unity on the basis of the adsorption data measured at 105 and 120 K.

Above 160 K the fractional coverage of the weakly bound precursor state is negligibly small ($\theta_p \ll 1$), and the pseudo-steady-state approximation $d\theta_p/dt \simeq 0$ may be assumed to hold. Therefore, eq 3 implies that

$$\theta_p = \frac{F}{k_d + k_r(1 - \theta_c)} \qquad (4)$$

The rate of adsorption, R_{ad}, into the chemisorbed state is obtained by substituting eq 4 into eq 2:

$$R_{ad} = \frac{d\theta_c}{dt} = \frac{F}{1 + \dfrac{k_d}{k_r(1 - \theta_c)}} \qquad (5)$$

The probability of adsorption is

$$P_{ad} = \frac{R_{ad}}{F} = \frac{1}{1 + \dfrac{k_d}{k_r(1 - \theta_c)}} \qquad (6)$$

(14) Weinberg, W. H. In *Kinetics of Interface Reactions*; Grunze, M., Kreuzer, H. J., Eds.; Springer-Verlag: Berlin, 1987; pp 94–124.

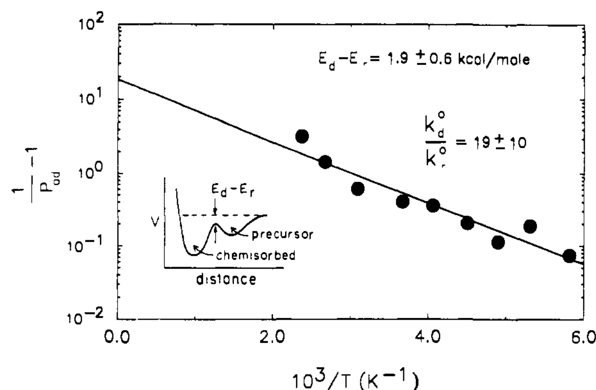

Figure 5. Arrhenius plot of ln $\{(1/P_{ad}) - 1\}$ vs $1/T$ for the adsorption of acetylene on Si(100). The slope is equal to $-(E_d - E_r)/R$ and the intercept to ln $(k_d°/k_r°)$; see eq 8 in the text. A schematic of the potential energy diagram is shown in the inset.

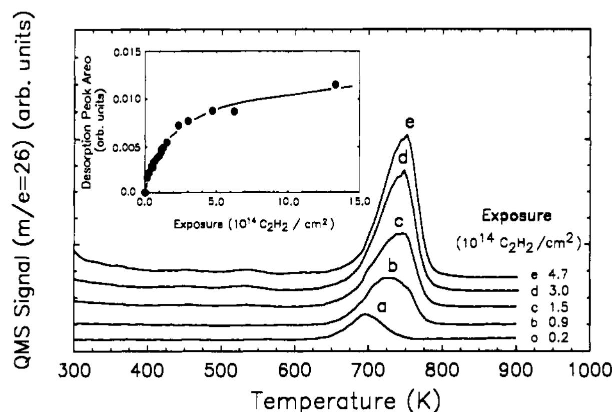

Figure 6. Temperature-programmed desorption of acetylene from Si(100)-(2×1). Adsorption temperature 120 K.

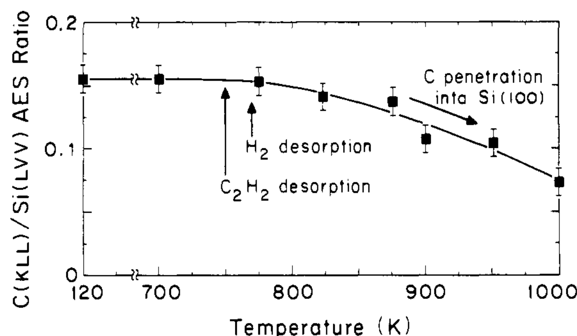

Figure 7. The change in carbon Auger intensity upon annealing to different temperatures. The error bars represent a $\pm 1\sigma$ deviation from the average of six AES measurements on the crystal.

By using the initial decrease in the reflected C_2H_2 signal upon removing the shutter (Figure 4), a measure of the initial adsorption probability at zero coverage, P_{ad}^0 ($t = 0$) where $P_{ad}^0 = \Delta_0/\Delta_1$, can be made at different crystal temperatures. From the measured values of P_{ad}^0 ($t = 0$), the ratio of the rate coefficients of desorption from the precursor state, k_d, to the rate of chemisorption (or reaction) from the precursor state, k_r, may be calculated by solving eq 6 for

$$\frac{k_d}{k_r} = \frac{1}{P_{ad}} - 1 \quad (7)$$

The temperature dependence of the ratio of the rates is given by

$$\frac{k_d}{k_r} = \frac{k_d°}{k_r°} \exp\{-(E_d - E_r)/RT\} \quad (8)$$

where $k_d°$ and $k_r°$ are the preexponential factors for precursor desorption and precursor reaction (chemisorption), respectively. The quantities E_d and E_r are the potential energy barriers for desorption and reaction from the precursor state. If the proposed mechanism is correct, an Arrhenius plot of ln $\{(1/P_{ad}^0) - 1\}$ vs $1/T$ should yield a straight line with a slope of $-(E_d - E_r)/R$ and an intercept of ln $\{k_d°/k_r°\}$. That analysis is shown in Figure 5. A value of $(E_d - E_r) = 1.9 \pm 0.6$ kcal mol^{-1} and a value of $k_d°/k_r° = 19 \pm 10$ were obtained for the adsorption of C_2H_2 on Si(100) over the temperature range 170–420 K. In this temperature range, measurable values of P_{ad}^0 exist below the onset temperature for desorption of chemisorbed C_2H_2 (see Figure 6).

C. Thermal Desorption of C_2H_2 from Si(100). Chemisorbed C_2H_2 on Si(100) exhibits two distinct reaction pathways upon increasing the silicon substrate temperature. One path leads to the desorption of C_2H_2 (a minor channel), whereas the major channel leads to the decomposition of C_2H_2 with subsequent hydrogen desorption and retention of carbon adatoms.

The thermal desorption spectra of acetylene from Si(100) reveals two desorption states, one at ~140 K and one at 690–740 K. The desorption peak at ~140 K is the desorption of molecularly adsorbed C_2H_2 on Si(100) from the precursor state; this feature was not studied in detail in this work. The desorption peak at ~690 K and above corresponds to the desorption of C_2H_2 from the chemisorbed state of C_2H_2 on Si(100). Figure 6 shows the thermal desorption spectra of C_2H_2 as a function of increasing C_2H_2 exposures.

From the thermal desorption spectra of chemisorbed acetylene on Si(100), the kinetic desorption parameters, activation energy (E_d), and preexponential factor ($k_d°$) have been obtained over a range of initial coverages of C_2H_2 using the Chan, Aris, and Weinberg (CAW)[15] analysis method assuming first-order kinetics and extrapolating to zero initial coverage. This extrapolation method is useful for removing coverage-dependent effects.[16] The estimated zero-coverage values for the activation energy and the preexponential factor for desorption from the chemisorbed state are $E_d° = 46.1 \pm 2.0$ kcal mol^{-1} and $k_d° = 2 \times 10^{13\pm1}$ s^{-1}, respectively. For the thermal desorption mass spectrometry reported here, the heating rate was $dT/dt = 0.87$ K s^{-1}, and the pumping time constant was estimated to be $\tau = 0.5$ s.

The possibility of surface reactions such as self-hydrogenation/dehydrogenation, oligomerization, and fragmentation could lead to a variety of desorbing products. A thorough search for desorbing species between 2 and 52 amu revealed that the *only* desorption products are acetylene and H_2. Acetylene desorption originates from nondissociatively chemisorbed acetylene on the silicon surface. Hydrogen originates from the desorption of molecular hydrogen, which is limited by C–H bond cleavage and will be discussed in the following section. These results suggest that surface oligomerization and/or hydrogenation to produce desorption products other than C_2H_2 and H_2 do not occur under the experimental conditions employed here. Surface reaction and/or fragmentation lead, in the major channel, to carbon-containing species that do not desorb but instead diffuse into the silicon lattice as the temperature is raised.

Auger spectroscopic measurements before and after thermal desorption were used to determine the amount of adsorbed acetylene that desorbs or reacts to form carbon adatoms. In Figure 7 the C(KLL)/Si(LVV) Auger ratios indicate that the amount of carbon remaining on the surface is a function of substrate temperature. The saturation coverage of C_2H_2 on Si(100) at 120 K results in a C(KLL)/Si(LVV) ratio of 0.15. Heating this saturation layer through the C_2H_2 desorption temperature results in an approximately 5% decrease in the carbon Auger signal as judged by the average data in Figure 7, indicating that the major reaction channel for chemisorbed acetylene involves retention of surface carbon for "Si–C" formation. Above the hydrogen de-

(15) Chan, C.-M.; Aris, R.; Weinberg, W. H. *Appl. Surf. Sci.* **1978**, *1*, 360.

(16) (a) Miller, J. B.; Siddiqui, H. R.; Gates, S. M.; Russell, J. N., Jr.; Yates, J. T., Jr.; Tully, J. C.; Cardillo, M. *J. Chem. Phys.* **1987**, *87*, 6725. (b) Niemantsverdrict, J. W.; Wandelt, K. *J. Vac. Sci. Technol.* **1988**, *A6*, 757.

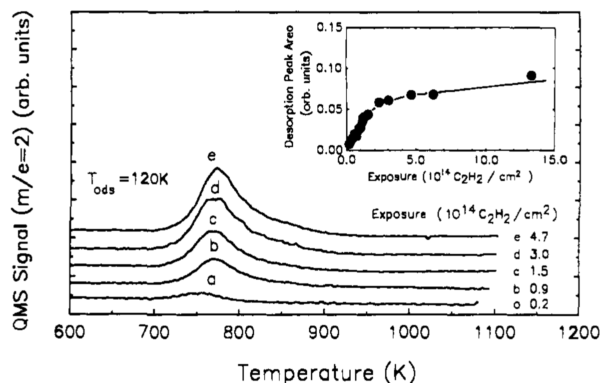

Figure 8. Thermal desorption of molecular hydrogen from acetylene on Si(100). The desorption of hydrogen from adsorbed acetylene on Si(100) indicates the thermal decomposition of acetylene on the silicon surface.

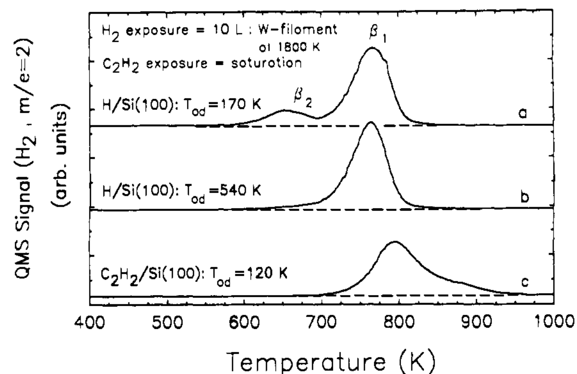

Figure 9. H_2 thermal desorption from atomic hydrogen and acetylene on Si(100). The silicon surface temperature during atomic hydrogen adsorption, T_{ad}, is indicated. The time integrated H_2 desorption yields, in arbitrary units (au), are (b) 3.17 au and (c) 2.47 au. The data were collected with a shielded QMS probing desorption only from the center of the silicon surface with a temperature ramp of dT/dt = 1.7 K s^{-1}. The "saturated" C_2H_2 exposure is 4.0×10^{15} C_2H_2 cm^{-2}.

sorption temperature, the carbon Auger signal begins to decrease as carbon diffuses into the bulk. Heating to 1000 K at a rate of ~1 K s^{-1}, followed by quenching to 120 K at a rate of ~5 K s^{-1}, gave a 60% reduction in the carbon measurable by Auger spectroscopy, where the remaining carbon is beyond the escape depth of the C(KLL) electrons (Figures 3 and 7). There are, therefore, two reaction pathways available to adsorbed acetylene on Si(100). Within the accuracy of the AES measurements, one pathway (minor <5%) leads to desorption of C_2H_2, and the second (major >95%) leads to surface reaction of acetylene with silicon to form carbon and hydrogen adatoms. Acetylene decomposition is followed by carbon diffusion into the bulk, which becomes measurable on the time scale of seconds above ~800 K. Qualitatively similar results have been reported for propylene on Si(100).[8]

D. Thermal Desorption of H_2 from C_2H_2 on Si(100). The origin of the desorbing molecular hydrogen may be determined by comparing the hydrogen thermal desorption kinetics from chemisorbed C_2H_2 with other adsorbates on silicon systems yielding H_2. The H_2 desorption kinetics from C_2H_2 on Si(100) are shown in Figure 8.

To compare the yield and kinetics of H_2 desorption from C_2H_2 chemisorbed on Si(100) with those of atomic hydrogen chemisorbed on Si(100), the experiments shown in Figure 9 were carried out. By comparing these experiments, (and also the result shown in Figure 8) it may be seen that H_2 desorption from C_2H_2 occurs at a temperature which is slightly higher than the desorption from pure atomic hydrogen on Si(100). This is probably due to the reaction-limited scission of C–H bonds followed by desorption of molecular hydrogen.

To compare the H_2 desorption yield from C_2H_2 on Si(100) with the H_2 desorption yield from a saturated monohydride phase of atomic hydrogen on Si(100), it is necessary to adsorb the atomic hydrogen at ~540 K to prevent the formation of di- and trihydrides during the adsorption of atomic hydrogen.[17,18] To adsorb atomic hydrogen, the Si(100) crystal was placed 3 cm from a tungsten spiral heated to 1800 K in a background H_2 (g) pressure of ~1×10^{-8} Torr. All the atomic hydrogen exposures in Figure 9 correspond to 10 langmuirs of H_2 at the tungsten spiral. As shown in Figure 9a this atomic hydrogen exposure at 170 K is sufficient to saturate the monohydride (β_1) and to form higher hydrides (β_2) on the Si(100) crystal. When the atomic hydrogen is adsorbed at 540 K there is no evidence for the formation of the higher hydrides (β_2), cf. Figure 9b, and the H_2 desorption yield from the monohydride phase may be compared to the H_2 desorption yield from a saturated coverage of C_2H_2 adsorbed on Si(100)-(2×1).

Curve c in Figure 9 was obtained from the decomposition of a monolayer of C_2H_2 on the Si(100) crystal. The integrated yield of H_2 in this case is 78% of that observed for the monohydride desorption (curve b) from a saturated surface of hydrogen atoms adsorbed at 540 K. If the crystal were perfect, 1 monolayer of di-σ-bonded C_2H_2 should produce a hydrogen yield equivalent to the H_2 yield from a saturated monohydride overlayer. However, two factors reduce the yield of H_2 from the decomposition of C_2H_2: (1) Natural defect sites on the Si(100)-(2×1) surface (10–20%) are known to be inactive for adsorption of unsaturated hydrocarbons.[6,8] (2) C_2H_2 does not quantitatively decompose to carbon and hydrogen on Si(100); about 5% of the C_2H_2 desorbs as C_2H_2 (cf. Figures 6 and 7).

IV. Discussion

A. Determination of Monolayer Coverage of C_2H_2 on Si(100). The ideal reconstructed Si(100)-(2×1) surface exposes 3.4×10^{14} Si_2 cm^{-2} as dimer sites. Our measurements of the absolute saturated monolayer coverage of C_2H_2 on Si(100) are of fundamental importance in establishing a structural model for the chemisorbed species. If the ideal Si(100)-(2×1) surface adsorbed one C_2H_2 per Si_2 dimer, then there would be two hydrogen atoms per Si_2 dimer. As shown above, we find that the yield of H_2 (g) from a saturated coverage of C_2H_2 is 78% of that from the saturated monohydride coverage. To account for all the hydrogen desorbing from the saturated C_2H_2 surface we must also include the 5% of the hydrogen desorbing as C_2H_2 (g). Therefore, the total yield of H_2 from the saturated acetylene coverage is approximately 83% of that from a saturated monohydride phase on Si(100)-(2×1).

The hydrogen yield measurement indicates that there is 0.83 C_2H_2 per Si_2 dimer for a saturated monolayer coverage and therefore suggests that approximately 17% of the surface silicon atom sites are defective (one silicon-vacancy defect implies the removal of one Si_2 dimer bonding site). This is in accordance with two observations: (1) The saturation coverage for chemisorption of unsaturated hydrocarbon molecules on Si(100) is diminished by the presence of defects introduced by ion bombardment.[6,8] (2) Scanning tunneling microscopy studies of Si(100)-(2×1) surfaces carefully prepared by annealing in ultrahigh vacuum exhibit ~10% surface defects.[19] A saturation coverage of one C_2H_2 per Si_2 dimer on the ideal Si(100)-(2×1) surface has also been deduced from absolute C_2H_2 coverage measurements reported elsewhere.[10]

B. Adsorption Kinetics for C_2H_2 on Si(100). The adsorption measurements suggest that C_2H_2 chemisorbs on Si(100) by way of a mobile precursor mechanism.[14] From the dependence of the rate of adsorption of C_2H_2 on substrate temperature given by eq 8, the difference in activation energy for desorption from the precursor and reaction from the precursor, ($E_d - E_r$), was determined to be 1.9 ± 0.6 kcal mol^{-1}. The low-temperature C_2H_2 thermal desorption feature, with T_p = 140 K, may be used to estimate the desorption energy from this precursor state. Using

(17) (a) Greenlief, C. M.; Gates, S. M.; Holbert, P. A. *J. Vac. Sci. Technol.* **1989**, *A7*, 1845. (b) Gates, S. M.; Kunz, R. R.; Greenlief, C. M. *Surf. Sci.* **1989**, *207*, 364.
(18) Cheng, C. C.; Yates, J. T., Jr. *Phys. Rev. B* **1991**, *43*, 4041.
(19) Hamers, R. J.; Tromp, R. M.; Demuth, J. E. *Phys. Rev. B* **1986**, *34*, 5343.

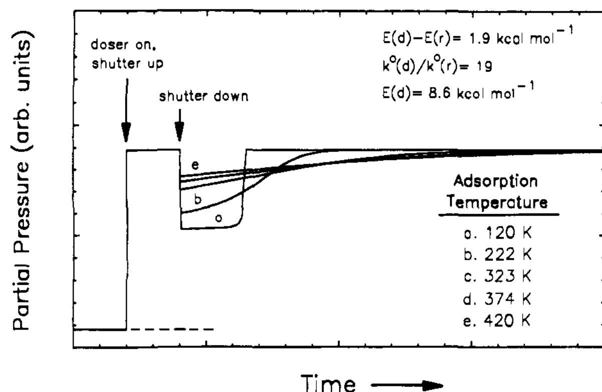

Figure 10. Rate of adsorption as predicted from the precursor-mediated adsorption model in which the intrinsic and extrinsic precursors are energetically equivalent. See text for assumptions and parameters.

first-order kinetics, using a heating rate of 1.4 K s^{-1}, and assuming a preexponential factor of 10^{13} s^{-1}, the desorption energy from this precursor state is calculated to be $E_d \cong 8.6$ kcal mol^{-1}. This desorption energy falls within the reported range for the heat of adsorption of acetylene on an inert surface (activated charcoal), with $10.8 \geq \Delta H_{ads} \geq 3.3$ kcal mol^{-1}.[20] Therefore, the activation energy for C_2H_2 chemisorption from the precursor is estimated to be $E_r \cong 6.7$ kcal mol^{-1}. In addition, we find that $k_d^\circ/k_r^\circ \approx 19$ (see Figure 5). This implies that the entropy of activation for desorption, $\Delta S_d^\ddagger$, is greater than the entropy of activation for reaction, $\Delta S_r^\ddagger$. This is an expected effect, since it is likely that the transition state for reaction will be more "localized" than that for desorption, given the specific steric requirements to form the di-σ-bonded chemisorbed state of C_2H_2 compared to those for desorption.

The behavior of the rate of adsorption of C_2H_2 on Si(100) as a function of coverage and temperature is shown by the partial pressure changes in C_2H_2 as seen in Figure 4. This behavior can be compared to the theoretically calculated adsorption curves in Figure 10. To obtain the theoretical adsorption curves, we assumed (1) $\theta_p \ll 1$; (2) the steady-state approximation $d\theta_p/dt = 0$ holds; (3) 0.45 of the available C_2H_2 flux intercepts the crystal; (4) a very high pumping speed exists; and (5) adsorbate–adsorbate interactions are negligible. In addition to the above assumptions, we allowed $(E_d - E_r) = 1.9$ kcal mol^{-1}; $k_d^\circ/k_r^\circ = 19$, $E_d = 8.6$ kcal mol^{-1}; $k_d \approx 10^{13}$ s^{-1}, and the partial pressure changes due to desorption from the precursor state are given by $\Delta P = F(1 - P_{ad})$ where F is the flux at the crystal and P_{ad} is given by eq 6.

As can be seen by comparing Figures 4 and 10, the precursor-mediated adsorption model, with the above assumptions, qualitatively describes the temperature and coverage dependency of C_2H_2 adsorption on Si(100). At low temperatures, $T < 140$ K, the precursor state can populate, refuting the assumptions 1 and 2 above. Therefore, the model is not appropriate at $T < 140$ K, which becomes obvious when comparing the theoretical and experimental adsorption curves at 120 K. An accurate description of the adsorption kinetics at low temperatures requires the solution of the two parametric inhomogeneous coupled differential eqs 2 and 3.

C. Structural Model of Chemisorbed Acetylene on Si(100)-(2×1). The hydrocarbon chemistry of the Si(100)-(2×1) surface is determined by the number, energetics, and geometric location of the surface dangling bonds. The number of available dangling bonds on the perfect Si(100)-(2×1) surface is 6.8×10^{14} cm^{-2}. On the perfect Si(100)-(2×1) surface the dangling bonds are arranged into dimer pairs,[19,21] as shown in Figure 11A.

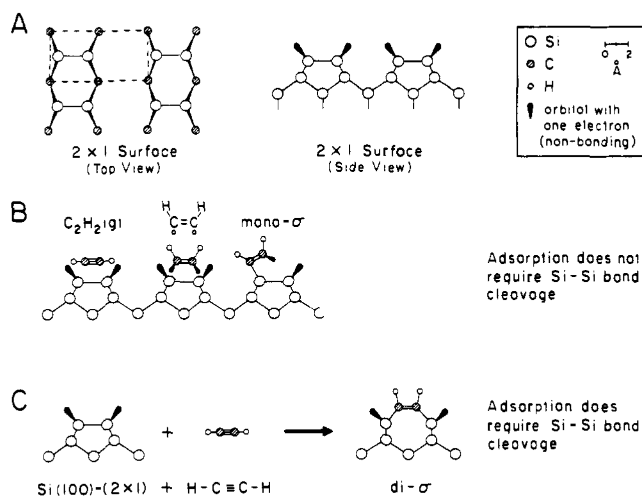

Figure 11. Model of Si(100)-(2×1) surface and C_2H_2 on Si(100) surface. (A) Clean Si(100) surface: top and side views, showing the (2×1) reconstruction. (B) Model for the adsorption of C_2H_2 on Si–Si dimer without Si–Si dimer bond cleavage. (C) Model for the adsorption of C_2H_2 on Si–Si dimer with Si–Si dimer bond cleavage. In this model, sp^2 hybridization of carbon is assumed for the di-σ species.

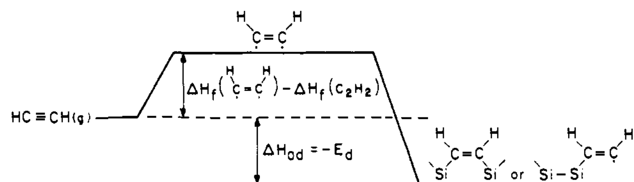

Figure 12. Thermochemical scheme for HC≡CH bonding to Si(100). Appropriate values of the energies are listed in Table I.

Adsorption of acetylene on Si(100)-(2×1) may be envisioned to occur by either mono-σ or di-σ attachment, as shown in Figure 11B,C. To bond with the silicon dangling bonds, the carbon sp-orbitals of acetylene rehybridize to sp^2-orbitals allowing a favorable overlap with the silicon sp^3-orbitals. In rehybridizing, the acetylene forms a diradical species with the relative dimensions and orbital orientation shown in Figure 11B.[22] The diradical may bond by either mono-σ or di-σ attachment as shown in Figure 11B,C. The only reasonable mechanism of di-σ attachment is one accompanied by cleavage of the Si-Si dimer bond allowing the diradical sp^2-orbitals and silicon sp^3-orbitals to be aligned appropriately as shown in Figure 11C. These geometrical considerations therefore suggest that acetylene adsorption will occur either via a mono-σ attachment (without breaking the Si–Si dimer) or via di-σ attachment with breaking the Si–Si dimer bond (cf. Figure 11B,C).

Using the van der Waals radius of acetylene ($r = 1.72 \times 10^{-8}$ cm[23]), we estimate that mono-σ attachment could produce up to two radical species per Si_2 dimer without overlapping of van der Waals spheres. This possible packing of mono-σ species would result in a saturation coverage of two C_2H_2 per Si_2 dimer, in disagreement with saturation coverage measurements made here (Figure 9) and elsewhere,[10] where one C_2H_2 per Si_2 dimer is proposed for a perfect Si(100)-(2×1) surface.

From the results of LEED and high-resolution electron energy loss spectrometric (HREELS) studies of C_2H_2 on Si(100)-(2×1), Nishijima et al.[24] suggested that the acetylenic carbon atoms rehybridize upon adsorption to form a di-σ surface species in which the Si-Si dimer bond does not cleave. Such di-σ bonding to the Si(100)-(2×1) surface without Si-Si bond cleavage is unlikely

(20) The heat of adsorption of acetylene on activated charcoal was calculated from the number of grams of acetylene adsorbed on 0.25 g of activated charcoal at different temperatures and pressures, as reported by Laukhof and Plank: Laukhof, W. L. S.; Plank, C. A. *J. Chem. Eng. Data* **1969**, *14*, 48. Our analysis of their data gave as a range for the heat of adsorption 10.8 kcal mol^{-1} (zero coverage limit) to 3.3 kcal mol^{-1} (the maximum reported coverage).

(21) Appelbaum, J. A.; Hamann, D. R. *Surf. Sci.* **1978**, *74*, 21.

(22) (HĊ═ĊH) diradical has been calculated to have the bond and angle dimensions nearly equivalent to that of ethylene. See: Wu, C. J.; Carter, E. A. *J. Phys. Chem.* **1991**, *95*, 8352.

(23) *Chemical Rubber Company Handbook of Chemistry and Physics*, 65th ed.; Weast, R. C., Ed.; CRC Press Inc.: Boca Raton, FL, 1984; p D-191.

(24) Nishijima, M.; Yoshinobu, J.; Tsuda, H.; Onchi, M. *Surf. Sci.* **1987**, *192*, 383.

Table I. Thermochemical Information regarding HC≡CH Adsorption on Si(100)

process	ΔH (kcal mol^{-1})	ref
$\Delta H_{ad}(C_2H_2)$	−46 [= $-E_d$(HC≡CH)]	this work[a]
$\Delta H_f(H\dot{C}{=}\dot{C}H)$	~138	b
$\Delta H_f(C_2H_2(g))$	54	c
$D°(H_3Si{-}CH_3)$	88	d
$D°((CH_3)_3Si{-}CH_3)$	89	d

[a] Assumes that the results in Figure 6 apply to desorption of HC≡CH from a normal Si_2 adsorption site. [b] ΔH estimated on the basis of the additivity rules for thermodynamic properties of molecules (Benson, S. W.; Buss, J. H. *J. Chem. Phys.* **1958**, *29*, 546). The calculated values are $\Delta H_f(C_2H_4)$ = 12 kcal mol^{-1}; $\Delta H_f(\cdot C_2H_3)$ = 70 kcal mol^{-1}; therefore, $\Delta H_f(\cdot C_2H_3) - \Delta H_f(C_2H_4)$ = 58 kcal mol^{-1}. By the additivity rules $\Delta H_f(:C_2H_2) \cong \Delta H_f(\cdot C_2H_3)$ + 58 kcal mol^{-1} ≃ 128 kcal mol^{-1}. Recent ab initio calculations give $\Delta H_f(:C_2H_2)$ = 138 ± 2 kcal mol^{-1}. See: Wu, C. J.; Carter, E. *J. Phys. Chem.* **1991**, *95*, 8352, which indicates that the additivity rules are somewhat inaccurate because of neglect of the triplet electron repulsion. [c] *Chemical Rubber Company Handbook of Chemistry and Physics*, 63rd ed.; Weast, R. C., Ed.; CRC Press Inc.: Boca Raton, FL, 1983, p D-98. [d] Walsh, R. *Acc. Chem. Res.* **1981**, *14*, 246.

due to the strain in the silicon lattice introduced upon chemisorption.

LEED studies, as a function of coverage, performed in these experiments (data not shown) and elsewhere[24] show that the (2×1) LEED pattern remains after C_2H_2 adsorption, although the LEED beams are broadened. These LEED results, coupled to the monolayer coverage measurements, indicate that the adsorbed acetylene layer must retain the (2×1) reconstruction. Our determination that one C_2H_2 per Si_2 dimer site constitutes the saturated monolayer is in accordance with this structural observation of (2×1) periodicity.

D. Thermochemical Model for C_2H_2 Adsorption on Si(100)-(2×1). The mono-σ and the di-σ attachment models for the adsorption of C_2H_2 on Si(100)-(2×1) can be assessed using thermochemical information available to us. Here we compare the two possibilities. Table I lists the information needed to make this comparison.

As shown in Figure 12, a thermochemical (a Born cycle) scheme may be devised to bind C_2H_2 to the surface, and from this scheme we may estimate the binding energy of C_2H_2 by mono-σ or di-σ adsorption.

In Figure 12 we recognize that $\Delta H_{ad}(C_2H_2) = -E_d(C_2H_2)$. Let $D(Si{-}C_2H_2)$ equal the energy of the chemical bond(s) between C_2H_2 and the Si(100) surface. We may write

$$D(Si{-}C_2H_2) = -\Delta H_{ad}(C_2H_2) + \Delta H_f(H\dot{C}{=}\dot{C}H) - \Delta H_f(C_2H_2(g)) \quad (9)$$

$$= 46 + 138 - 54 = +130 \text{ kcal mol}^{-1}$$

Comparing the results of eq 9 with the values for $D°$(Si–C) in Table I, we see that mono-σ bonding of C_2H_2 to silicon would involve the production of a single Si–C bond with 130 kcal mol^{-1} of bond energy, which is far above the 88–89 kcal mol^{-1} bond energy of model compounds containing the Si–C bond (Table I).

For di-σ bonding of C_2H_2 to a Si_2 dimer site, a more favorable Si–C bond energy is involved. Desorption from the di-σ configuration also involves the energy gain due to the reformation of the Si–Si dimer bond. Theoretical calculations of the energy gained from dimerization varies from 38.5 kcal mol^{-1}[25] to 47.5 kcal mol^{-1}.[26] Using the average Si–Si dimer bond energy, the desorption from a di-σ configuration with concerted reformation of the Si–Si dimer bond then gives

$$D(Si_2{-}C_2H_2) + 43 \pm 4.5 = 2D°(Si{-}C)$$

$$= 173 \pm 4.5 \text{ kcal mol}^{-1}$$

$$D°(Si{-}C) \cong 86.5 \pm 2.3 \text{ kcal mol}^{-1}$$

Since the calculated Si–C bond energy is in close accord with known Si–C energies (88–89 kcal mol^{-1}, Table I), the di-σ C_2H_2 bonding to Si(100) is preferred according to this thermodynamic argument. Indeed, minimization of strain in the silicon lattice would cause one to *expect* that the carbon–silicon bond strength in the surface bond would be somewhat less than that in the model compounds.

V. Conclusions

The following features of C_2H_2 adsorption, surface bonding, and thermal decomposition on Si(100)-(2×1) have been found:

1. Acetylene adsorbs on Si(100)-(2×1) via a mobile precursor mechanism. At low temperatures (~105–120 K) the initial probability of adsorption is unity.

2. The difference in the activation energy for desorption from the precursor and reaction from the precursor to the chemisorbed state ($E_d - E_r$) was determined to be 1.9 kcal mol^{-1}, indicating that a molecule in the precursor state will favor reaction over desorption on energetic grounds. On entropic grounds, desorption is favored as reflected by the measured value of $k_d°/k_r° \cong 19$. From thermal desorption measurements, the activation energy for desorption from the precursor state was estimated to be $E_d \simeq 8.6$ kcal mol^{-1}, giving an activation energy for C_2H_2 reaction with Si(100)-(2×1) from the precursor state of $E_r \simeq 6.7$ kcal mol^{-1}.

3. The chemisorbed C_2H_2 species forms a saturated monolayer with one C_2H_2 per Si_2 dimer site.

4. Thermochemical arguments concerning the bonding of C_2H_2 to the Si_2 dimer site indicate that a di-σ surface species is involved. The formation of the di-σ-bonded C_2H_2 is accompanied by Si–Si dimer bond cleavage.

5. Chemisorbed C_2H_2 undergoes two different thermally activated reactions: A minor pathway (<5%) involves desorption of C_2H_2 with an activation energy of 46 kcal mol^{-1}, and a major pathway involves dissociation of chemisorbed C_2H_2, forming "Si–C".

6. Above 800 K, surface carbon formed from C_2H_2 decomposition begins to diffuse into the Si(100) crystal.

Acknowledgment. We would like to acknowledge the assistance of L. Clemen in some of the exploratory experiments and discussions that led to this work. We also acknowledge with thanks the support of this work by the Office of Naval Research. Discussions with Professor Emily Carter are gratefully acknowledged. W.H.W. gratefully acknowledges support from the National Science Foundation via grant CHE-9003553.

(25) Abraham, F. F.; Batra, I. P. *Surf. Sci.* **1985**, *163*, L752.
(26) Pandey, K. C. In *Proceedings of the Seventeenth International Conference on the Physics of Semiconductors*; Chodi, D. J., Harrison, W. A., Eds.; Springer: New York, 1985; p 55.